ACS chemical biology

Letters

Cite This: ACS Chem. Biol. 2019, 14, 2546−2552

pubs.acs.org/acschemicalbiology

# Affinity-Based Protein Profiling Reveals Cellular Targets of Photoreactive Anticancer Inhibitors

Nan Ma,[†] Zhi-Min Zhang,[†] Jun-Seok Lee,[§] Ke Cheng,[†] Ligen Lin,[∥] Dong-Mei Zhang,[†] Piliang Hao,*[,‡] Ke Ding,*[,†] Wen-Cai Ye,*[,†] and Zhengqiu Li*[,†]

[†]School of Pharmacy, Jinan University, Guangzhou City Key Laboratory of Precision Chemical Drug Development, International Cooperative Laboratory of Traditional Chinese Medicine, Modernization and Innovative Drug Development Ministry of Education (MOE) of People's Republic of China, 601 Huangpu Avenue West, Guangzhou 510632, China

[‡]School of Life Science and Technology, ShanghaiTech University, 393 Middle Huaxia Road, Shanghai 201210, China

[§]Molecular Recognition Research Center, Korea Institute of Science and Technology (KIST), Seoul 136-791, Korea

[∥]State Key Laboratory of Quality Research in Chinese Medicine, Institute of Chinese Medical Sciences, University of Macau, Taipa, Macau 999078, China

Supporting Information

**ABSTRACT:** Affinity-based protein profiling has proven to be a powerful method in target identification of bioactive molecules. Here, this technology was applied in two photoreactive anticancer inhibitors, arenobufagin and HM30181. Using UV irradiation, these photoreactive reagents can covalently cross-link to target proteins, leading to a covalent binding with target proteins. Moreover, the cellular on/off targets of these two molecules, including ATP1A1, MDR1, PARP1, DDX5, NOP2, RAB6A, and ERGIC1 were first identified by affinity-based protein profiling and bioimaging approaches. The protein hit, PARP1, was further validated to be involved in the function of the anticancer effects.

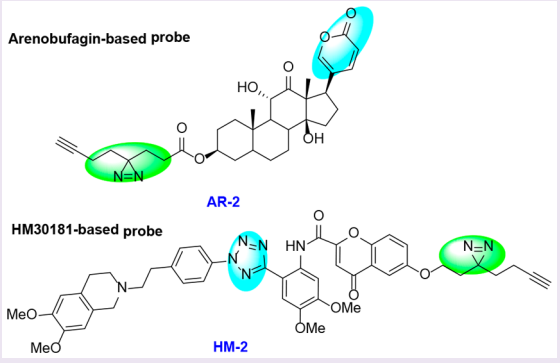


Photoaffinity labeling (PAL), a powerful tool for *in situ* investigation of noncovalent ligand−receptor interactions, plays an essential role in various areas such as chemical biology, medicinal chemistry, and structural biology.[1−3] The key feature of this method is that in response to UV irradiation, a covalent bond is formed between the photo-cross-linker and residues in the protein receptor. This leads to conversion of reversible interactions to irreversible interactions. When such a permanent conversion happens in anticancer agents, it can prolong drug action and, at the same time, eliminate the residual activity of unbound inhibitors.[4] Common photo-cross-linkers include diazirine, benzophenone, and arylazide, all of which have different photo-cross-linking mechanisms.[5,6] The most popular application of PAL is that it is coupled with quantitative proteomics, also termed affinity-based protein profiling (AfBP), to identify and characterize the cellular targets of bioactive molecules. This also enables mapping of the binding sites of a ligand with receptors, thus facilitating a better understanding of the underlying mechanisms of action.[7] However, one issue with this method is the uncertainty of photo-cross-linking yield when a photoprobe labels target proteins in their native environment.[8] To alleviate this issue, we have recently developed a new photo-cross-linker, diaryltetrazole, which demonstrates remarkable properties of improved stability, labeling specificity and efficiency, and a unique cross-linking mechanism.[9−11] In recent years, a suite of minimalist bioorthorgonal handle-containing photo-cross-linkers or linkers has been developed by us for reversible and irreversible inhibitors, respectively.[12−16] These linkers have not only significantly improved the probe labeling efficiency but also have enabled simultaneous proteome profiling and bioimaging studies, thereby providing opportunities for accurate target identification.

It has been observed that the anticancer molecules arenobufagin and HM30181 have a photo-cross-linker, α-pyrone[17] and diaryltetrazole,[9−11] respectively. Therefore, they are photoreactive anticancer inhibitors. Arenobufagin,[18,19] a representative bufadienolide, is the major active component in the traditional Chinese medicine of Chan'su, displaying a broad spectrum of anticancer activity. Over the years, extensive efforts have been devoted to understand the mechanism of its anticancer behavior, but to date, only one potential target, $Na^+$,$K^+$-ATPase (ATP1A1), has been discovered and still needs to be further validated.[20] This obscure mechanism of action has become a major problem in the development of arenobufagin.[21] HM30181, a third generation P-gp multidrug

Received: October 1, 2019
Accepted: November 14, 2019
Published: November 19, 2019






DOI: 10.1021/acschembio.9b00784
ACS Chem. Biol. 2019, 14, 2546−2552

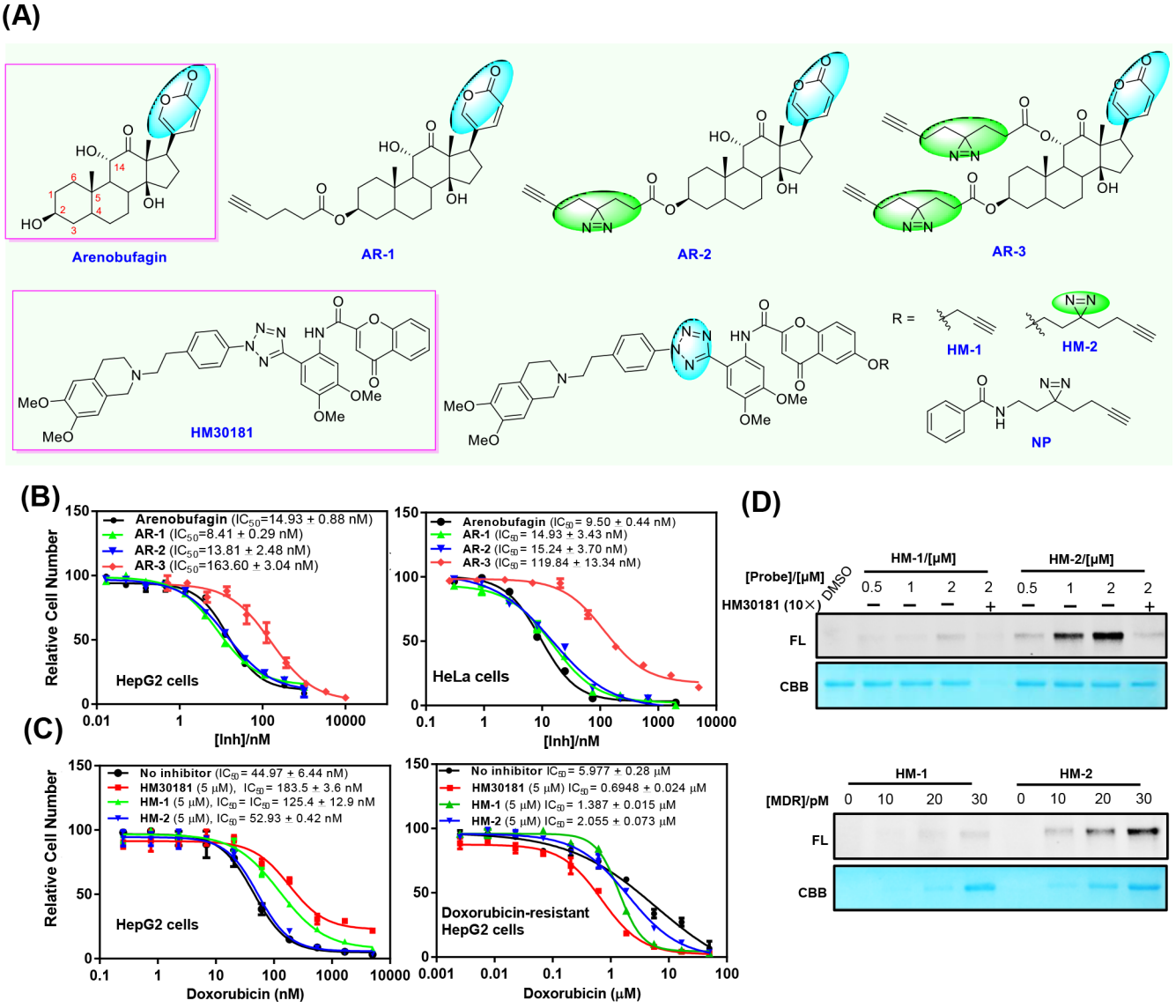


**Figure 1.** (A) Structures of arenobufagin, HM30181, and corresponding photoreactive/negative probes (NP). (B) $IC_{50}$ values of the arenobufagin and **AR-1**/**-2**/**-3** against various cancer cells. (C) Activity profiles of HM30181 and **HM-1**/**-2** against doxorubicin-resistant and doxorubicin-sensitive HepG2 cells. $IC_{50}$ values were obtained from the treatment of doxorubicin. (D) Concentration-dependent labeling of recombinant MDR1 with **HM-1**/**-2**. FL = in-gel fluorescence scanning. CBB = Coomassie gel.

resistance gene (MDR1) inhibitor,[22] is now in clinical trials, but toxicity and side effects have been observed[23] and could be accounted for by off-target binding. Weissleder et al. have recently developed a suite of fluorescent probes based on this molecule for imaging of MDR1 expression and inhibition,[24] but the cellular targets are still unknown. In an attempt to disclose the underlying cellular targets of both of these anticancer agents, two sets of photoprobes containing an alkyne handle and a minimalist photo-cross-linker, respectively, were created for comparison.

Previous structure−activity relationships indicated that modification of the C-2 hydroxyl group of arenobufagin and the chromone of HM30181 does not compromise their bioactivities.[25,26] Thus, an alkyne handle and a minimalist photo-cross-linker were incorporated into amenable sites to produce the probes **AR-1**/**AR-2** and **HM-1**/**HM-2** (Figure 1A), respectively. The synthesis was accomplished by standard coupling reactions following previously reported procedures with yields of ∼50% (Supporting Information, Schemes S1−S5). During the synthesis of **AR-2**, a side-product containing two minimalist photo-cross-linkers (**AR-3**) was isolated as a control probe (Scheme S3). To assess whether the introduction of these linkers affects bioactivities of these probe molecules, we first evaluated their antiproliferative activity against the corresponding cancer cells using a CCK8 assay; the parent inhibitors were tested concurrently as positive controls. As shown in Figure 1B, C, **AR-1** and **AR-2** showed comparable inhibition of arenobufagin against both HeLa and HepG2 cancer cells. In contrast, a weak inhibition was observed from **AR-3**, suggesting that the C-14 hydroxyl group is essential for probe binding. As expected, **HM-1** and **HM-2** are capable of displaying a similar potency to HM30181 against common and doxorubicin-resistant HepG2 cells by targeting MDR1. These results proved that the probes, **AR-1**/**AR-2** and **HM-1**/**HM-2**, largely preserved the bioactivities of the parent inhibitors.

Next, we carried out chemoproteomics and bioimaging studies with the probes to evaluate their labeling performance



DOI: 10.1021/acschembio.9b00784
ACS Chem. Biol. 2019, 14, 2546−2552

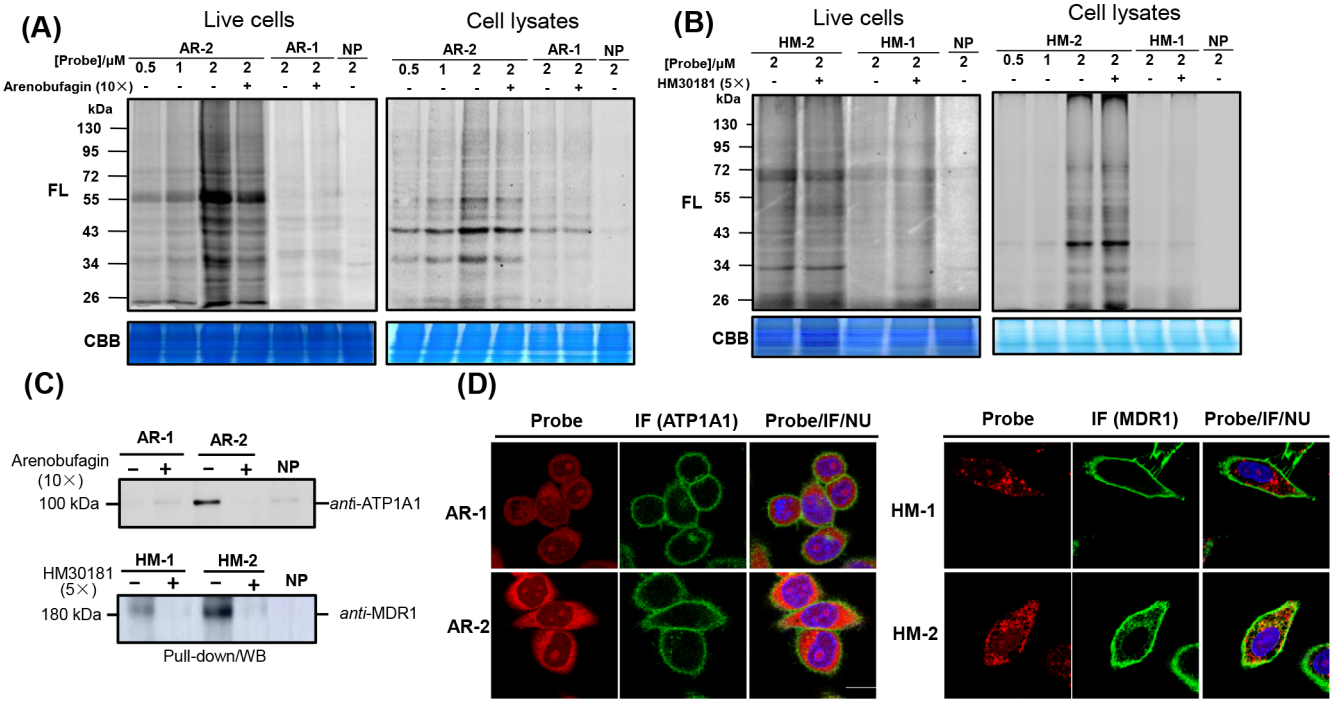


**Figure 2.** Proteome reactivity profiles of (A) live HeLa cells and cell lysates with **AR-1**/**AR-2**, (B) doxorubicin-resistant HepG2 cells, and cell lysates with **HM-1**/**HM-2**, in the presence or absence of corresponding parent inhibitors. (C) Pull-down/WB results for target validation of **AR-1**/**AR-2** (100 nM) and **HM-1**/**HM-2** (5 $\mu$M) in live HeLa and doxorubicin-resistant HepG2 cells, respectively. (D) Live cell imaging of HeLa and doxorubicin-resistant HepG2 cells with **AR-1**/**AR-2** (2 $\mu$M) and **HM-1**/**HM-2** (1 $\mu$M), respectively. IF = immunofluorescence. Scale bar = 10 $\mu$m.

in both *in situ* and *in vitro* settings. First labeling profiles of recombinant MDR1 with **HM-1** and **HM-2** were carried out to test their labeling efficiency *in vitro*. After incubation of the probes in various concentrations with different amounts of protein for 30 min, the mixture was exposed to UV light for 10 min and then conjugated with TAMRA-$N_3$. The proteins labeled in this way were separated by SDS-PAGE and visualized by in-gel fluorescence scanning. As shown in Figure 1D, **HM-2** is capable of labeling the target protein at a probe concentration as low as 0.5 $\mu$M, whereas **HM-1**-treated samples only gave distinct labeling bands at a probe concentration of 2 $\mu$M. Moreover, MDR1 protein at levels as low as 10 pM can be successfully detected by **HM-2** at a 2 $\mu$M probe concentration, but not in **HM-1**-treated samples, indicating that the minimalist-linker containing probe, **HM-2**, possesses excellent labeling capabilities. Subsequently, labeling profiles of live cells and cell lysates were performed to assess the performance of these probes in labeling of complex cellular proteomes. Upon incubation of **AR-1**/**AR-2** and **HM-1**/**HM-2** with live HeLa and doxorubicin-resistant HepG2 cells for 4 h, respectively, the cells were irradiated with UV light and then lysed; the resulting cell lysates were conjugated with TAMRA-$N_3$, separated by SDS-PAGE, and then visualized. As shown in Figure 2A and B, **AR-2** and **HM-2** consistently generated stronger labeling bands than those of **AR-1** and **HM-1** in both live cells and cell lysates, suggesting that **AR-2** and **HM-2** are more efficient than **AR-1** and **HM-1** in labeling the cellular targets. Interestingly, these *in situ* profiles were different from the results of *in vitro* proteome profiling (Figure 2A and B), which proved that the probes interact with different sets of proteins between in live cells and in cell lysates. After a click reaction with biotin-$N_3$, the labeled proteomes were affinity purified and validated by pull-down/WB experiments, which demonstrated that **AR-2** and **HM-1**/**2** can successfully label the known targets, ATP1A1 and MDR1, at concentrations as low as 100 nM and 5 $\mu$M probe concentration, respectively (Figure 2C). The labeling profiles and pull-down/WB bands were abolished in the presence of excess parent inhibitors, demonstrating that the probes successfully labeled the intended cellular targets of the original inhibitors.

Subsequently, bioimaging experiments were carried out to assess whether the affinity-based probes can track the cellular distribution of parent inhibitors. HeLa and doxorubicin-resistant HepG2 cells were treated with **AR-1**/**AR-2** and **HM-1**/**HM-2**, respectively, and this was followed by UV irradiation to initiate photo-cross-linking. The cells were then fixed, permeabilized, and clicked with TAMRA-$N_3$ under previously established optimal click chemistry conditions,[9−16] then they were imaged. Strong fluorescence signals were observed, located mainly outside of the nucleus in **AR-1** and **AR-2** treated cells, and the fluorescence signals of **HM-1** and **HM-2** treated cells were located mainly in the cell membrane (Figure 2D). The fluorescence signals produced from the probes can cover the fluorescence of target proteins, ATP1A1 and MDR1, generated from immunofluorescence (IF) experiments with the corresponding antibodies (Figure 2D). The different locations between the probes and corresponding target proteins were mainly in the cytosol and can be attributed to the existence of off-targets. Consistent with the trend of labeling profiles, samples treated with **AR-2** or **HM-2** gave stronger fluorescence signals than cells treated with **AR-1** or **HM-1**, and the fluorescence intensity decreased sharply in the presence of excess parent inhibitors (arenobufagin or HM30181, Figure S2, Supporting Information). Control imaging experiments with negative probe (NP, Figure 1A) and DMSO under the same conditions gave minimal background fluorescence compared with probe-treated cells (Figure S3). Taken together, these competitive labeling



DOI: 10.1021/acschembio.9b00784
*ACS Chem. Biol.* 2019, 14, 2546−2552

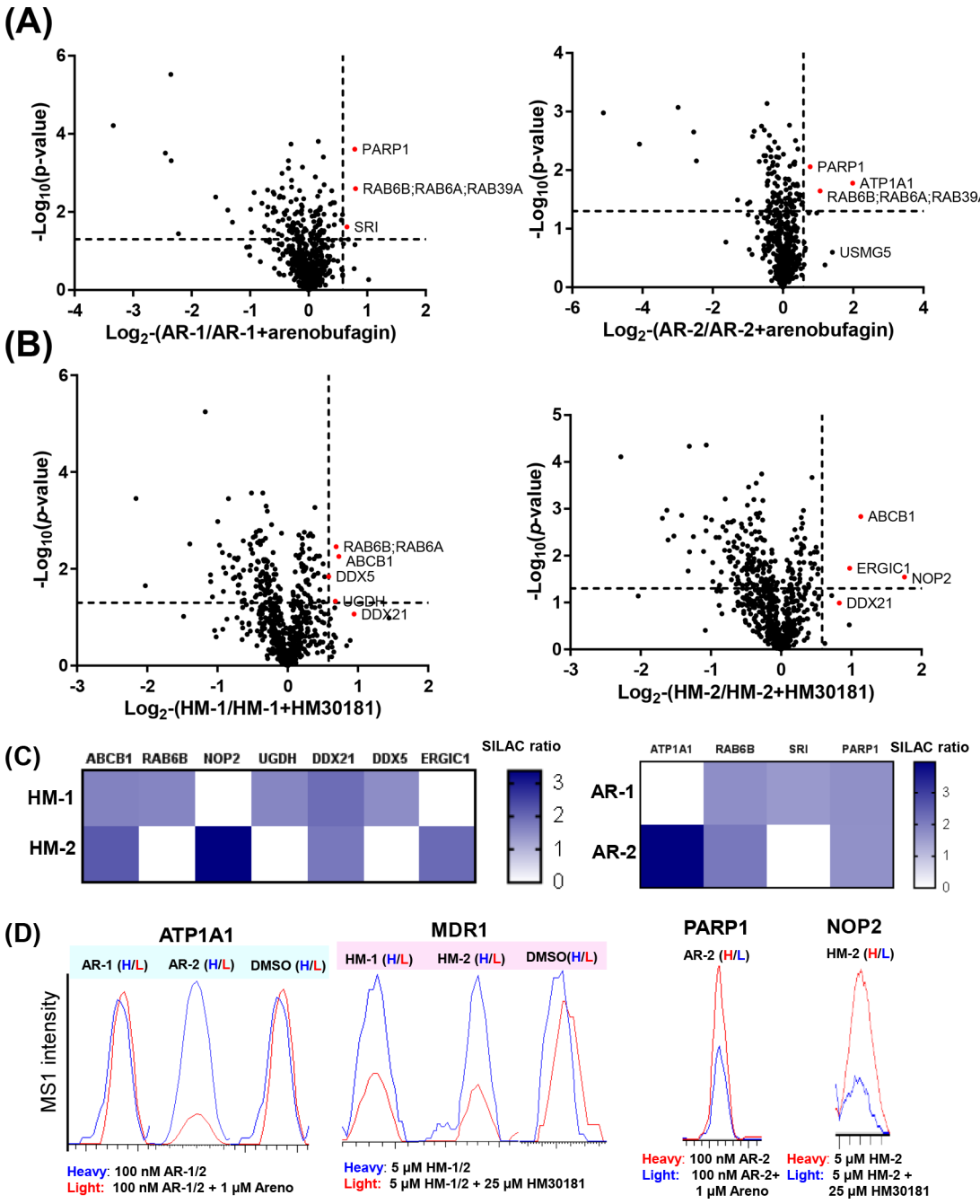


**Figure 3.** (A) Quantitative mass spectrometry-based profiling of **AR-1/-2** (100 nM) in the presence of excess papent inhibitors (10×), AR = arenobufagin. (B) Quantitative mass spectrometry-based profiling of **HM-1/-2** (5 $\mu$M) in the presence of excess papent inhibitors (5×), HM = HM30181. See Tables S1 and S2 for more complete presentations of the quantitative proteomic data. (C) Heatmap of high-occupancy protein targets of arenobufagin and HM30181. (D) Extracted MS1 chromatographs for representative peptides of ATP1A1 and MDR1, repectively (ATP1A1: NVEDLSGGELQR, $m/z$ 658.819; MDR1: IVEIPFNSTNK, $m/z$ 631.336), ATP1A1 and MDR1 shown for **AR-1/-2** ± 10× arenobufagin and **HM-1/-2** ± 5× HM30181 competition experiments, respectively. PARP1: GGAAVDPDSGLEHSAHVLEK. NOP2: NTGVILANDANAER. See Tables S1 and S2 for more complete presentations of the quantitative proteomic data.

profiles and live-cell imaging experiments proved that the minimalist linker-containing probes, **AR-2** and **HM-2**, are more efficient than **AR-1** and **HM-1** in labeling intended cellular targets.

We proceeded to identify cellular on/off targets of arenobufagin and HM30181 by large-scale chemoproteomics experiments. Low probe concentrations (100 nM for **AR-1**/**AR-2** and 5 $\mu$M for **HM-1**/**HM-2**) were used to reduce nonspecific binding and simulate the drug action. Similar to the procedures described above, SILAC (stable isotope labeling by amino acids) labeled HeLa and doxorubicin-resistant HepG2 cells were treated with **AR-1**/**AR-2** and **HM-1**/**HM-2**, respectively, and this was followed by UV irradiation. Upon cell lysis, the resulting probe-labeled proteomes were affinity-purified and identified by LC-MS/MS. Control experiments with the probes in the presence of the corresponding parent inhibitors or with DMSO were carried out concurrently, and served to distinguish between real targets and background



DOI: 10.1021/acschembio.9b00784
ACS Chem. Biol. 2019, 14, 2546−2552

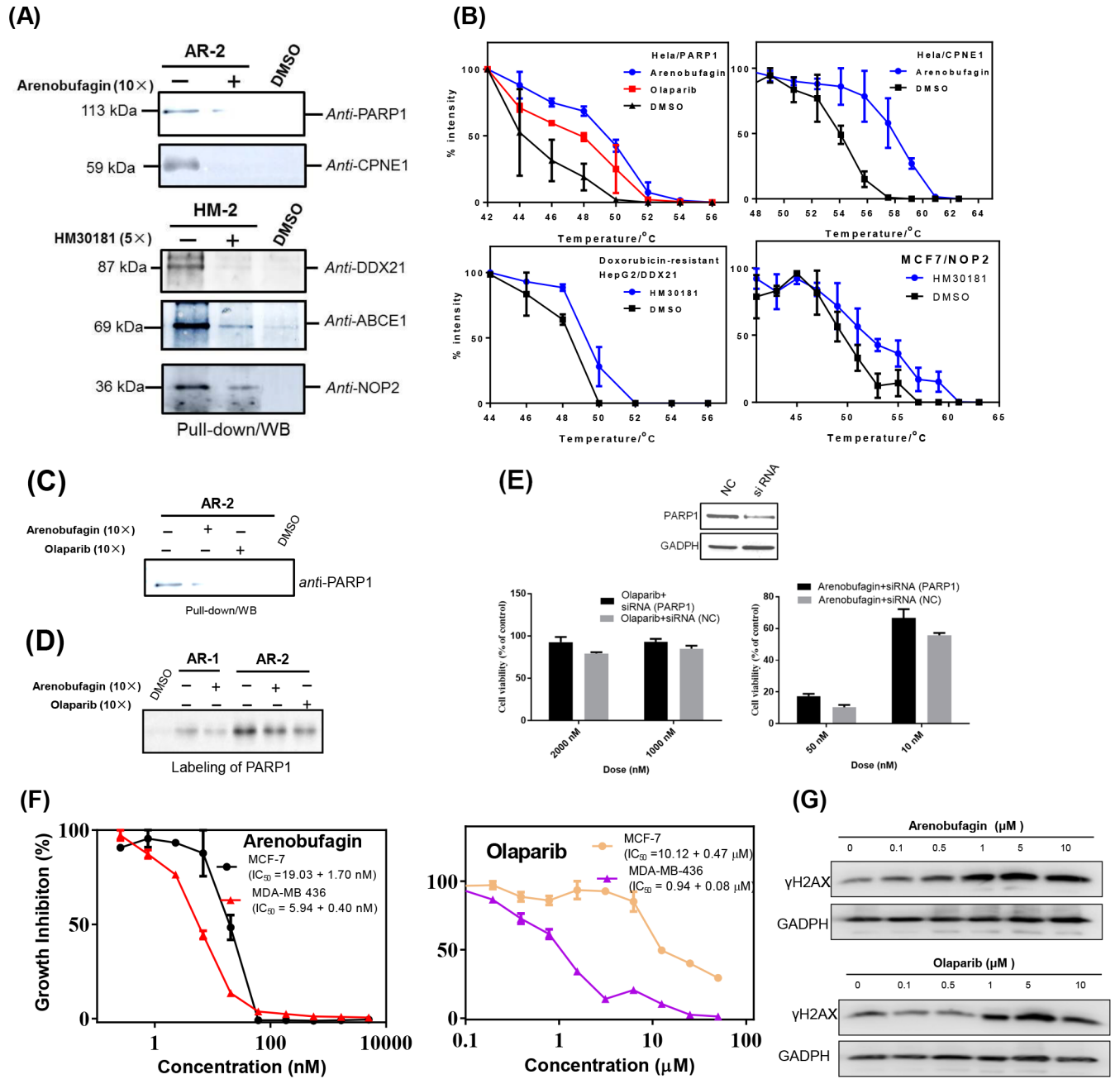


**Figure 4.** (A) Target validation of CPNE1, PARP1, DDX21, ABCE1 and NOP2 by pull-down/WB in the presence or absence of parent inhibitors (100 nM and 5 $\mu$M probe concentration for AR-2 and HM-2, respectively). (B) Thermal shift binding assay of arenobufagin with Hela cells and HM30181 with doxorubicin-resistant HepG2 cells. Olaparib, a known PARP1 inhibitor, was used as a positive control. (C) Pull-down/WB in the presence or absence of arenobufagin or Olaparib (100 nM probe concentration). (D) Labeling of recombinant PARP1 with **AR-1**/**-2** in the presence or absence of arenobufagin or Olaparib (2 $\mu$M probe concentration). (E) Antiproliferative effects of arenobufagin and Olaparib against HeLa cells in the presence or absence of siRNA PARP1, cells treated with scrambled siRNA are a negative control (NC). (F) Antiproliferative effects of arenobufagin and Olaparib against MDA-MB 436 and MCF-7 cells. (G) Arenobufagin and Olaparib increased the levels of $\gamma$-H2AX in MDA-MB 436 cells.

labeling. The identified protein hits were analyzed by corresponding volcano plots as a $\log_2$ of the competition ratio (probe/probe with excess competitors) against statistical significance ($-\log_{10} p$ value). Proteins with a $p$ value less than 0.05 and a competition ratio (probe/probe with excess competitors) greater than 1.5 were considered to be significant hits. On the basis of these criteria, three protein hits were identified by **AR-1** and **AR-2**, and four and three protein hits were produced by **HM-1** and **HM-2**, respectively (Figure 3A,B and Tables S1 and S2, Supporting Information). Consistent with the pull-down/WB results (Figure 2C), the known target of arenobufagin, ATP1A1 (sodium/potassium-transporting ATPase subunit alpha-1) can only be detected by **AR-2** (Figure 3A), but the ABCB1 (MDR1, multidrug resistance protein 1) was successfully detected from both **HM-1** and **HM-2** treated samples (Figure 3B). This further confirmed that arenobufagin can directly target ATP1A1 *in situ*. Interestingly, most of the SILAC ratios produced by **AR-2**



DOI: 10.1021/acschembio.9b00784
ACS Chem. Biol. 2019, 14, 2546−2552

and **HM-2** were higher than those of **AR-1** and **HM-1** (Figure 3C, Tables S1 and S2), reaffirming that the minimalist linker-containing probes are more capable than probes with inherent photo-cross-linkers in labeling cellular targets. In addition to known targets, several unknown targets of arenobufagin, including PARP1, RAB6A/6B/39A, and SRI, were also identified. Among these proteins, PARP1 (Poly [ADP-ribose] polymerase 1) and RAB6A/6B/39A (Ras-related protein Rab-6A/6B/39A) were simultaneously detected by both **AR-1** and **AR-2**, indicating the high reliability of the identification. Rab proteins serve an important role in endocytosis and biosynthetic protein transport; it is also a modulator of the unfolded protein response and implicated in Alzheimer's disease.[27,28] PARP1 is an attractive anticancer drug target by anchoring DNA damage.[29] The identified off-targets of HM30181 include NOP2, DDX5, ERGIC1, RAB6A/6B, and UCDH. NOP2 (probable 28S rRNA (cytosine(4447)-C(5))-methyltransferase) is associated with cell proliferation.[30] ERGC1 (endoplasmic reticulum golgi intermediate compartment 1) is a potential drug target in prostate and gastric cancer,[31,32] and DDX5 (probable ATP-dependent RNA helicase DDX5) is strongly implicated in the tumorigenesis, invasiveness, and metastasis, as well as the proliferation of several cancer types.[33] These protein hits might be the reason underlying the anticancer effects of arenobufagin and HM30181.

Considering that PARP1 is a well-estabilished target for drug development, functional validations were further carried out with olaparib, a potent PARP1 inhibitor, as a positive control. PARP1 and several protein hits with high SILAC ratios, including CPNE1, NOP2, DDX21, and ABCE1, were validated by pull-down/WB and thermal shift binding assay (Figure 4A,B). Binding of arenobufagin induced a larger thermal shift of PARP1 than olaparib (Figure 4B). The pull-down/WB bands of PARP1 can be competed away by treatment of excess olaparib or arenobufagin (Figure 4C); a similar phenomenon was also observed from the labeling of recombinant PARP1 protein (Figure 4D). These lines of evidence suggest direct binding between arenobufagin and PARP1 protein. When knockdown of the PARP1 by siRNA transfection in HeLa cells occurred, it led to reduced antiproliferative effects (Figure 4E), indicating that PARP1 is essential for keeping the anticancer activities of arenobufagin. An antiproliferation assay demonstrated that arenobufagin displayed remarkably higher inhibition efficacy toward PARP1 sensitive cells (BRCA1-deficient MDA-MB 436) than the nomal cancer cells (BRCA1/2-proficient MCF-7; Figure 4F).[34] As shown in Figure 4G, treatment with arenobufagin at various concentrations led to significantly enhanced levels of $\gamma$-H2AX, a molecular marker for DNA double-strand breaks, in MDA-MB 436 cells.[35] Taken together, these data prove that PARP1 is a functional target of arenobufagin.

In conclusion, affinity-based protein profiling was employed in cellular target identification of photoreactive anticancer inhibitors arenobufagin and HM30181. A series of previously known and unknown protein hits from arenobufagin or HM30181 were identified by a quantitative proteomics approach. The identified protein hits here provide direct evidence that arenobufagin directly targets ATP1A1 *in situ*. Further functional validations indicate that PARP1 is an off-target of arenobufagin. These protein hits might be useful clues for the understanding of drug action and potential toxic effects.

## ■ ASSOCIATED CONTENT

### Supporting Information

The Supporting Information is available free of charge at https://pubs.acs.org/doi/10.1021/acschembio.9b00784.

Sections on methodology, Figures S1−S4, Tables S1 and S2 (PDF)

## ■ AUTHOR INFORMATION


### Corresponding Authors

*E-mail: haopl@shanghaitech.edu.cn.
*E-mail: dingke@jnu.edu.cn.
*E-mail: chywc@aliyun.com.
*E-mail: Pharmlzq@jnu.edu.cn.

### ORCID

Jun-Seok Lee: 0000-0003-3641-1728
Piliang Hao: 0000-0002-3632-1573
Ke Ding: 0000-0001-9016-812X
Zhengqiu Li: 0000-0002-0433-2147


### Notes

The authors declare no competing financial interest.

## ■ ACKNOWLEDGMENTS

Funding was provided by National Natural Science Foundation of China (81803389, 21602079, 21877050), Science and Technology Program of Guangdong Province (2017A050506028, 2019B151502025), Science and Technology Program of Guangzhou (201704030060, 201805010007), China Postdoctoral Science Foundation (No.2017M622923), and the Ph.D. Start-up Fund of Natural Science Foundation of Guangdong Province, China (NO. 2018A030310651). We thank S. Q. Yao (NUS, Singapore) for the invaluable suggestions and support on this work.

## ■ REFERENCES


(1) Kotzyba-Hibert, F., Kapfer, I., and Goeldner, M. (1995) Recent trends in photoaffinity labeling. *Angew. Chem., Int. Ed. Engl. 34*, 1296−1312.

(2) Das, J. (2011) Aliphaticdiazirines as photoaffinity probes for proteins: recent developments. *Chem. Rev. 111*, 4405−4417.

(3) Dubinsky, L., Krom, B. P., and Meijler, M. M. (2012) Diazirine based photoaffinity labeling. *Bioorg. Med. Chem. 20*, 554−570.

(4) Képiró, M., Várkuti, B. H., Bodor, A., Hegyi, G., Drahos, L., Kovács, M., and Málnási-Csizmadia, A. (2012) Azidoblebbistatin, a photoreactive myosin inhibitor. *Proc. Natl. Acad. Sci. U. S. A. 109*, 9402−9407.

(5) Murale, D. P., Hong, S. C., Haque, M. M., and Lee, J. S. (2016) Photo-affinity labeling (PAL) in chemical proteomics: a handy tool to investigate protein-protein interactions (PPIs). *Proteome Sci. 15*, 14.

(6) Yang, P., and Liu, K. (2015) Activity-based protein profiling: recent advances in probe development and applications. *ChemBioChem 16*, 712−724.

(7) Su, Y., Ge, J., Zhu, B., Zheng, Y.-G., Zhu, Q., and Yao, S. Q. (2013) Target identification of biologically active small molecules via in situ methods. *Curr. Opin. Chem. Biol. 17*, 768−775.

(8) Smith, E., and Collins, I. (2015) Photoaffinity labeling in target- and binding-site identification. *Future Med. Chem. 7*, 159−183.

(9) Cheng, K., Lee, J. S., Hao, P., Yao, S. Q., Ding, K., and Li, Z. (2017) Tetrazole-based probes for integrated phenotypic screening, affinity-based proteome profiling, and sensitive detection of a cancer biomarker. *Angew. Chem., Int. Ed. 56*, 15044−15048.

(10) Li, Z., Qian, L., Li, L., Bernhammer, J. C., Huynh, H. V., Lee, J. S., and Yao, S. Q. (2016) Tetrazole photoclick chemistry: reinvestigating its suitability as a bioorthogonal reaction and potential applications. *Angew. Chem., Int. Ed. 55*, 2002−2006.




DOI: 10.1021/acschembio.9b00784
*ACS Chem. Biol.* 2019, 14, 2546−2552

(11) Guo, H., Xu, J., Hao, P., Ding, K., and Li, Z. (2017) Competitive affinity-based proteome profiling and imaging to reveal potential cellular targets of betulinic acid. *Chem. Commun. 53*, 9620−9623.
(12) Zhu, D., Guo, H., Chang, Y., Ni, Y., Li, L., Zhang, Z.-M., Hao, P., Xu, Y., Ding, K., and Li, Z. (2018) Cell- and tissue-based proteome profiling and dual imaging of apoptosis markers with probes derived from venetoclax and idasanutlin. *Angew. Chem., Int. Ed. 57*, 9284−9289.
(13) Li, Z., Hao, P., Li, L., Tan, C. Y. J., Cheng, X., Chen, G.Y. J., Sze, S. K., Shen, H.-M., and Yao, S. Q. (2013) Design and synthesis of minimalist terminal alkyne-containing diazirine photo-crosslinkers and their incorporation into kinase inhibitors for cell- and tissue-based proteome profiling. *Angew. Chem., Int. Ed. 52*, 8551−8556.
(14) Li, Z., Wang, D., Li, L., Pan, S., Na, Z., Tan, C. Y. J., and Yao, S. Q. (2014) Minimalist" cyclopropene-containing photo-cross-linkers suitable for live-cell imaging and affinity-based protein labeling. *J. Am. Chem. Soc. 136*, 9990−9998.
(15) Guo, C., Chang, Y., Wang, X., Zhang, C., Hao, P., Ding, K., and Li, Z. (2019) Minimalist linkers suitable for irreversible inhibitors in simultaneous proteome profiling, live-cell imaging and drug screening. *Chem. Commun. 55*, 834.
(16) Guo, H., and Li, Z. (2017) Developments of bioorthogonal handle-containing photo-crosslinkers for photoaffinity labeling. *MedChemComm 8*, 1585−1591.
(17) Battenberg, O. A., Nodwell, M. B., and Sieber, S. A. (2011) Evaluation of $\alpha$-pyrones and pyrimidones as photoaffinity probes for affinity-based protein profiling. *J. Org. Chem. 76*, 6075−6087.
(18) Zhang, D. M., Liu, J. S., Deng, L. J., Chen, M. F., Yiu, A., Cao, H. H., Tian, H. Y., Fung, K. P., Kurihara, H., Pan, J. X., and Ye, W. C. (2013) Arenobufagin, a natural bufadienolide from toad venom, induces apoptosis and autophagy in human hepatocellular carcinoma cells through inhibition of PI3K/Akt/mTOR pathway. *Carcinogenesis 34*, 1331−1342.
(19) Li, M., Wu, S., Liu, Z., Zhang, W., Xu, J., Wang, Y., Liu, J., Zhang, D., Tian, H., Li, Y., and Ye, W. C. (2012) Arenobufagin, a bufadienolide compound from toad venom, inhibits VEGF-mediated angiogenesis through suppression of VEGFR-2 signaling pathway. *Biochem. Pharmacol. 83*, 1251−1260.
(20) Yue, Q., Zhen, H., Huang, M., Zheng, X., Feng, L., Jiang, B., Yang, M., Wu, W., Liu, X., and Guo, D. (2016) Proteasome inhibition contributed to the cytotoxicity of arenobufagin after its binding with Na, K-ATPase in human cervical carcinoma HeLacells. *PLoS One 11*, No. e0159034.
(21) Chen, L., Mai, W., Chen, M., Hu, J., Zhuo, Z., Lei, X., Deng, L., Liu, J., Yao, N., Huang, M., Peng, Y., Ye, W., and Zhang, D. (2017) Arenobufagin inhibits prostate cancer epithelial-mesenchymal transition and metastasis by down-regulating $\beta$-catenin. *Pharmacol. Res. 123*, 130−142.
(22) Kwak, J. O., Lee, S. H., Lee, G. S., Kim, M. S., Ahn, Y. G., Lee, J. H., Kim, S. W., Kim, K. H., and Lee, M. G. (2010) Selective inhibition of MDR1 (ABCB1) by HM30181 increases oral bioavailability and therapeutic efficacy of paclitaxel. *Eur. J. Pharmacol. 627*, 92−98.
(23) Kim, T. E., Lee, H., Lim, K. S., Lee, S., Yoon, S. H., Park, K. M., Han, H., Shin, S. G., Jang, I. J., Yu, K. S., and Cho, J. Y. (2014) Effects of HM30181, a P-glycoprotein inhibitor, on the pharmacokinetics and pharmacodynamics of loperamide in healthy volunteers. *Br. J. Clin. Pharmacol. 78*, 556−564.
(24) Sprachman, M. M., Laughney, A. M., Kohler, R. H., and Weissleder, R. (2014) In vivo imaging of multidrug resistance using a third generation MDR1 inhibitor. *Bioconjugate Chem. 25*, 1137−1142.
(25) Deng, L. J., Wang, L. H., Peng, C. K., Li, Y. B., Huang, M. H., Chen, M. F., Lei, X. P., Qi, M., Cen, Y., Ye, W. C., Zhang, D. M., and Chen, W. M. (2017) Fibroblast activation protein $\alpha$ activated tripeptidebufadienolideantitumor prodrug with reduced cardiotoxicity. *J. Med. Chem. 60*, 5320−5333.
(26) Köhler, S. C., and Wiese, M. (2015) HM30181 derivatives as novel potent and selective inhibitors of the breast cancer resistance protein (BCRP/ABCG2). *J. Med. Chem. 58*, 3910−3921.
(27) Huang, H., Jiang, Y., Wang, Y., Chen, T., Yang, L., He, H., Lin, Z., Liu, T., Yang, T., Kamp, D. W., Wu, B., and Liu, G. (2015) miR-5100 promotes tumor growth in lung cancer by targeting Rab6. *Cancer Lett. 362*, 15−24.
(28) Elfrink, H. L., Zwart, R., Cavanillas, M. L., Schindler, A. J., Baas, F., and Scheper, W. (2012) Rab6 is a modulator of the unfolded protein response: implications for Alzheimer's disease. *J. Alzheimer's Dis. 28*, 917−929.
(29) Helleday, T., Petermann, E., Lundin, C., Hodgson, B., and Sharma, R. A. (2008) DNA repair pathways as targets for cancer therapy. *Nat. Rev. Cancer 8*, 193−204.
(30) Wada, H., Yeh, E. T., and Kamitani, T. (2000) A Dominant-negative UBC12 Mutant Sequesters NEDD8 and Inhibits NEDD8 Conjugation. *J. Biol. Chem. 275*, 17008−17015.
(31) Wang, F. R., Wei, Y. C., Han, Z. J., He, W. T., Guan, X. Y., Chen, H., and Li, Y. M. (2017) Aberrant DNA-PKcs and ERGIC1 expression may be involved in initiation of gastric cancer. *World J. Gastroenterol. 23*, 6119−6127.
(32) Vainio, P., Mpindi, J. P., Kohonen, P., Fey, V., Mirtti, T., Alanen, K. A., Perälä, M., Kallioniemi, O., and Iljin, K. (2012) High-throughput transcriptomic and RNAi analysis identifies AIM1, ERGIC1, TMED3 and TPX2 as potential drug targets in prostate cancer. *PLoS One 7*, No. e39801.
(33) Nyamao, R. M., Wu, J., Yu, L., Xiao, X., and Zhang, F. M. (2019) Roles of DDX5 in the tumorigenesis, proliferation, differentiation, metastasis and pathway regulation of human malignancies. *Biochim. Biophys. Acta, Rev. Cancer 1871*, 85−98.
(34) Menear, K. A., Adcock, C., Boulter, R., Cockcroft, X. L., Copsey, L., Cranston, A., Dillon, K. J., Drzewiecki, J., Garman, S., Gomez, S., Javaid, H., Kerrigan, F., Knights, C., Lau, A., Loh, V. M. J., Matthews, I. T., Moore, S. O., O'Connor, M. J., Smith, G. C., and Martin, N. M. (2008) 4-[3-(4-cyclopropanecarbonylpiperazine-1-carbonyl)-4-fluorobenzyl]-2H-phthalazin-1-one: a novel bioavailable inhibitor of poly(ADP-ribose) polymerase-1. *J. Med. Chem. 51*, 6581−6591.
(35) Ye, N., Chen, C. H., Chen, T., Song, Z., He, J. X., Huan, X. J., Song, S. S., Liu, Q., Chen, Y., Ding, J., Xu, Y., Miao, Z. H., and Zhang, A. (2013) Design, synthesis, and biological evaluation of a series of benzo[de][1,7]naphthyridin-7(8H)-ones bearing a functionalized longer chain appendage as novel PARP1 inhibitors. *J. Med. Chem. 56*, 2885−2903.


DOI: 10.1021/acschembio.9b00784
*ACS Chem. Biol.* 2019, 14, 2546−2552